IC Test Structures for Multilayer Interconnect Stress Determination

Stephen A. Smee, Michael Gaitan, Donald B. Novotny, Yogendra Joshi, and David L. Blackburn

***Abstract*—A new method for measuring strain in multilayer integrated circuit (IC) interconnects is presented. This method utilizes process compatible MEMS-based test structures and is applied to the determination of longitudinal interconnect stress in a standard dual-metal-layer CMOS process. Strain measurements are shown to be consistent for an array of similar test structures. Stress values, calculated from constitutive relations, are in good agreement with published results.**

***Index Terms*—CMOS, IC interconnect, mechanical stress, MEMS, micromachining, test structures.**

I. Introduction

AS INTEGRATED CIRCUIT (IC) device sizes shrink, intrinsic and thermo-mechanical stresses in interconnects are an ever increasing reliability concern [1]–[3]. Increasing device density leads to high-density multilayer interconnects with narrow, high aspect ratio (height/width), metal lines. The corresponding increase in thermo-mechanical stress resulting from these trends increases the probability of stress related failure through mechanisms such as electromigration, stress-migration, and delamination. As a result, methods to measure and model interconnect stress are needed to develop processes that reduce stress and enable the manufacture of reliable future generation IC's.

To date, research has almost exclusively focused on stress determination and stress-related failure in simple single-layer metallization. This restriction to single-layer studies stems largely from a paucity of strain measurement techniques with sufficient spatial resolution to resolve individual layers of a multilayer system.

In this letter, a set of CMOS compatible micromachined test structures are demonstrated for the measurement of strain in multilayer interconnects. The basic test structure is a variant of the fixed-fixed beam structure investigated previously for strain measurement in homogeneous thin films [4]. The focus of this work is the application of these new test structures to the determination of longitudinal interconnect stress in a dual-metal-layer CMOS process.

Manuscript received March 6, 1999; revised June 25, 1999. This work was supported by the NIST National Semiconductor Metrology Program. The review of this letter was arranged by Editor H.-H. Vuong.

S. A. Smee and Y. Joshi are with the Department of Mechanical Engineering, University of Maryland, College Park, MD 20742 USA(e-mail: smee@piper.eeel.nist.gov).

M. Gaitan, D. B. Novotny, and D. L. Blackburn are with the National Institute of Standards and Technology, Semiconductor Electronics Division, Gaithersburg, MD 20899 USA.

Publisher Item Identifier S 0741-3106(00)00439-0.

II. Fixed–Fixed Beam Test Structures

The use of a buckled beam for determining the compressive stress in a thin film has been investigated before [4]. The basic principle is illustrated in Fig. 1(a). A beam shaped section of the film is created using MEMS processing techniques and the mechanically released section buckles due to the compressive film stress. Strain is then calculated from measurements of the maximum beam deflection V_m, and the beam length L. It can be shown [5] that the deflection profile for this beam is

$$y(x) = \frac{V_m}{2}\left(1 - \cos\frac{2\pi x}{L}\right). \tag{1}$$

This technique is extended here to the measurement of average strain in dielectric/interconnect composite films. Average strain measurements, from a set of test structures with different cross sections, are combined with constitutive relations and a force balance expression to determine the longitudinal stress in the interconnect and dielectric.

This type of test structure is ideal for our purpose because the dielectric/interconnect composite film is typically in compression and V_m is very sensitive to axial strain. In addition, the deflection profile is very insensitive to stress gradients across the thickness of the film.

III. Test Structure Design and Fabrication

Test structures were designed and fabricated to measure the longitudinal strain in dielectric/interconnect composite films. Four beam cross sections, representative of single- and double-layer interconnects, were investigated [see Fig. 1(b)]. The four cross sections were repeated in an array of varying length beams with nominal lengths, ranging between 50 and 400 μm, in 25 μm increments. An array was used to ensure strain measurements are independent of test structure length. Thicknesses for the Metal-1 and Metal-2 layers are 0.6 and 1.05 μm, respectively. Linewidths are nominally 10 μm, with the exception of the Metal-1 layer of beam (iv), where it is 14 μm. Though the linewidths here are considerably wider than state-of-the-art, they are sufficient for our purpose, which is proof of concept.

The test structures described were fabricated in a 1.2-μm CMOS process available through a commercial foundry. Openings left in each SiO_2 layer form the beam sidewalls and act as "etch openings" for the post-process micromachining step. A pulsed xenon difluoride etching process [6] was used to remove isotropically the silicon beneath each beam, mechanically releasing it from the underlying substrate. The compressive stress in the released film leads to the buckled profile shown in Fig. 1.

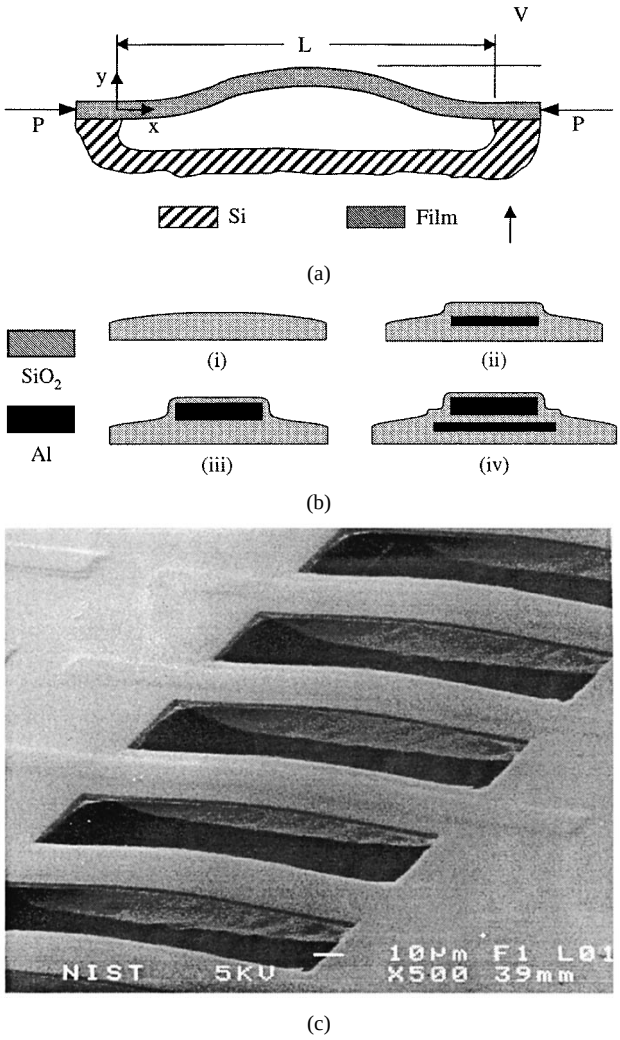

Fig. 1. (a) Schematic representation of a micromachined fixed-fixed beam test structure; (b) beam cross sections: (i) SiO_2, (ii) SiO_2 and Al from the first metallization layer (SiO_2/Metal-1), (iii) SiO_2 and Al from the second metallization layer (SiO_2/Metal-2), and (iv) SiO_2 and Al from both metallization layers (SiO_2/Metal-1/Metal-12); and (c) SEM micrograph showing composite FFB test structures.

A SEM micrograph of the completed test structures is shown in Fig. 1(c).

Layer thickness and cross section geometry were obtained from SEM measurements. Material properties [8] are taken to be: $E_{\mathrm{SiO_2}} = 72$ GPa, $\nu_{\mathrm{SiO_2}} = 0.16$, $E_{\mathrm{Al}} = 69$ GPa, and $\nu_{\mathrm{Al}} = 0.33$, where E and ν are Young's modulus and Poisson's ratio, respectively.

IV. Mathematical Formulation

A general expression for the unreleased film strain, $\langle\varepsilon\rangle$, suitable for either homogeneous or composite beam cross sections, has been derived from the definition of uniaxial strain $\varepsilon = \Delta\ell/\ell$ and the deflection profile (1). Using beam theory and (1), this relation can be expressed as

$$\langle\varepsilon\rangle = -\left(\frac{\pi}{L}\right)^2\left[\frac{V_m^2}{4} + \frac{4\overline{EI}}{\overline{EA}}\right]$$
$$\overline{EI} = \sum_{j=1}^{n} E_j I_j, \quad \overline{EA} = \sum_{j=1}^{n} E_j A_j \tag{2}$$

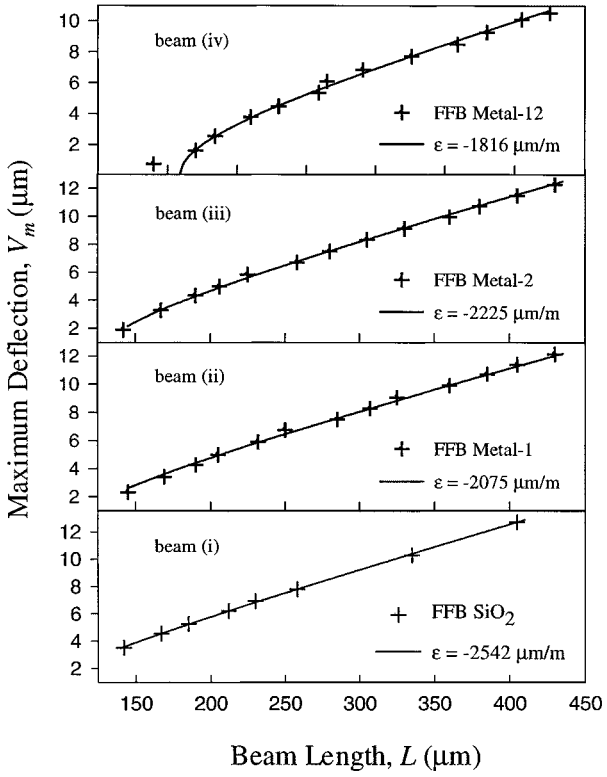

Fig. 2. Maximum deflection, V_m, as a function of test structure length, L; measurement uncertainty is ±5 μm in length and ±0.1 μm in deflection.

TABLE I
Stress and Strain Values Calculated from Test Structure Data. Uncertainty in the Stress and Strain Values Presented is ±7 MPa and ±70 μm/m, Respectively

Beam	(i)	(ii)	(iii)	(iv)
$\langle\varepsilon\rangle$ (µm/m)	-2542	-2075	-2225	-1816
σ_{SiO_2} (MPa)	-218	-218	-218	-218
σ_{M1} (MPa)	—	229	—	220
σ_{M2} (MPa)	—	—	-20	-20

where

$\overline{EI}$ composite bending;
$\overline{EA}$ axial stiffness;
E_j elastic modulus;
I_j moment of inertia;
A_j area of the j material in the cross section.

Furthermore, it is assumed that the materials behave elastically when released; often a reasonable assumption given that SiO_2 exhibits little plasticity and confined metal films exhibit yield strengths considerably higher than their bulk values [9].

The average stress, $\langle\sigma\rangle$, in the unreleased film can be determined from the constitutive relation

$$\langle\sigma\rangle = E_{ave}\langle\varepsilon\rangle, \quad E_{ave} = \frac{1}{A_{tot}}\sum_{j=1}^{n} E_j A_j \tag{3}$$

where E_{ave} and A_{tot} are the average modulus and total cross sectional area, respectively. The stress in the individual mate-

rials of the unreleased composite sections shown in Fig. 1(b) can be calculated from the force balance equation

$$\sum_{j=1}^{n} \sigma_j A_j = \langle \sigma \rangle A_{tot} \tag{4}$$

where σ_j is the stress in the jth material. The stress in the homogeneous SiO_2 beam, beam (i) of Fig. 1(b), can be calculated directly from (3). Substituting this value into (4) for beams (ii) and (iii) yields the stress for Metal-1 and Metal-2, respectively. Likewise, substituting SiO_2 and Metal-2 stress values into the force balance for beam (iv), the stress in the underlying Metal-1 interconnect can be calculated. Similarly, the stress value for Metal-1, calculated from beam (ii) data, can be used to calculate the stress in Metal-2 of beam (iv).

V. Results and Discussion

Measurements of deflection profile were taken from the test structures using an optical profilometer and are in good agreement with that predicted by (1). Compressive strains have been calculated, using (2), for each of the four test structures depicted in Fig. 1(b). In Fig. 2, maximum deflections, V_m, are plotted as a function of beam length along with values predicted from (2) for a constant strain value. From this data it is evident that, regardless of beam length, strain measurements are consistent. Interconnect and dielectric stresses, determined from these strain values, are tabulated in Table I; the negative signs indicate compression.

It is difficult to make a true quantitative comparison between these values and those reported in the literature due to variability and limited knowledge of processing conditions. Moreover, the processing conditions here are unknown since the foundry considers this information proprietary. Despite this, some comments can be made concerning the validity of these numbers.

1) The assumption that the stress in the blanket SiO_2 film is equal to the stress in the SiO_2 passivating the Al lines, beams (ii)–(iv), is reasonable [7].
2) The assumption that the Metal-2 stress of beam (iii) is identical to that of beam (iv) is reasonable, as suggested by Shen [8].
3) The compressive stress in SiO_2 (218 MPa) agrees reasonably well with the value of 270 MPa reported by Fang and Wickert [4].
4) The tensile stress in Metal-1 of beam (ii) (229 MPa) and beam (iv) (220 MPa) are in good agreement with the average value, 300 MPa, reported by Wang *et al.* [10] using microbeam X-ray diffraction, and extrapolation from experimental data by Yeo *et al.* [7].
5) The decrease in Metal-1 stress, which accompanies the increase in linewidth (from 10 to 14 μm), is consistent with numerical [11] and experimental [7] studies.
6) The very low compressive stress in Metal-2 is puzzling. The low magnitude may be due to the very thin, 0.3-μm, overlying passivation. The compressive nature of the stress is difficult to explain devoid, of processing information.

In general, the stress values determined from the test structures presented here are in good agreement with experimental studies reported in the literature.

VI. Conclusion

Based on the experimental results, MEMS-based test structures appear to be a viable solution to the multilayer-interconnect stress determination problem. Aside from the ability to determine stress in multilayer interconnects, ease of measurement and compatibility with standard IC processing make this an attractive alternative to existing measurement techniques. Additional test structures are currently being developed for the determination of transverse stress, and it is envisioned that, in the near future, mechanical test structures such as these will be incorporated into test chips along with their electrical counterparts.

Acknowledgment

The authors would like to thank J. Small of NIST for his assistance with the layer thickness measurements.

References

[1] J. Curry, G. Fitzgibbon, Y. Guan, R. Muollo, G. Nelson, and A. Thomas, *22nd Annu. Proc. Reliability Physics* , 1984, p. 6.
[2] P. R. Besser, T. N. Marieb, and J. C. Bravman, "Strain relaxation and *in-situ* observation of voiding in passivated aluminum alloy lines," in *Mat. Res. Soc. Symp.*, vol. 309, 1993, pp. 181–186.
[3] P. S. Ho, I.-S. Yeo, C. N. Liao, S. G. H. Anderson, and H. Kawasaki, "Thermal stress and relaxation behavior of Al(Cu) submicron interconnects," in *Int. Conf. Solid-State and Integrated Circuit Technol.*, 1995, pp. 408–412.
[4] W. Fang and J. A. Wickert, "Post buckling of micromachined beams," *J. Micromech. Microeng.*, vol. 4, pp. 116–122, 1994.
[5] S. P. Timoshenko and J. M. Gere, *Theory of Elastic Stability*. New York: McGraw-Hill, 1961, pp. 54–55; 204.
[6] P. B. Chu, J. T. Chen, R. Yeh, G. Lin, J. Huang, B. A. Warneke, and K. Pister, "Controlled pulsed-etching with xenon difloride," *Transducers '97*, June 16–19, 1997.
[7] I.-S. Yeo, S. G. H. Anderson, P. S. Ho, and C. K. Hu, "Characteristics of thermal stresses in Al(Cu) fine lines—Part II: Passivated line structures," *J. Appl. Phys.*, vol. 72, no. 2, pp. 953–961, 1995.
[8] Y.-L. Shen, "Thermal stresses in multilevel interconnections: Aluminum lines at different levels," *J. Mater. Res.*, vol. 12, no. 9, pp. 2219–2222, 1997.
[9] M. Murakami, T.-S. Kuan, and I. A. Blech, *Treatise on Materials Science and Technology*. New York: Academic, 1982, vol. 24, p. 163.
[10] P.-C. Wang, G. S. Cargill III, I. C. Noyan, E. G. Liniger, C.-K. Hu, and K. Y. Lee, "Thermal and electromigration strain distributions in 10 μm wide aluminum conductor lines measured by X-ray microdiffraction," in *Mat. Res. Soc. Symp.*, vol. 473, 1997, pp. 273–278.
[11] A. I. Sauter and W. D. Nix, "Thermal stresses in aluminum lines bonded to substrates," *IEEE Trans. Comp., Hybrids, Manufact. Technol.*, vol. 15, pp. 594–600, 1992.